UDC 551.243

ACTIVE FAULTS IN THE WEST OF THE LUT BLOCK (CENTRAL IRAN)

A. Rashidi[1], H. Kianimehr[2], S. Shafieibafti[3], A. Mehrabi[3], R. Derakhshani[3,4]

[1] *International Institute of Earthquake Engineering and Seismology, Tehran, Iran*
[2] *Iranian Seismological Center, Institute of Geophysics, University of Tehran, Tehran, Iran*
[3] *Shahid Bahonar University of Kerman, Kerman, Iran*
[4] *Utrecht University, Utrecht, the Netherlands*
Corresponding authors: A. Rashidi (rashidi@iiees.ac.ir) & R. Derakhshani (r.derakhshani@uu.nl)

The western margin of the Lut Block, in southeastern Iran, has experienced many historical and instrumental destructive earthquakes where 13 earthquakes, from 1977 to 2020, totally had surface rupture with a length of roughly 207 km. In this study, we indicated active tectonic evidence of the fundamental faults based on the DEM terrain interpretation, and satellite data analysis with field data. We investigated surface evidence related to the activity of the faults and their depth characteristics. Our results of the geometric-kinematic characteristic of the faults have general applications in describing strike-slip faults, development of releasing, and restraining bends in positive flower structures.

Keywords: active faults, seismic activity, geomorphological evidence, releasing and restraining bends, Central Iran.

Introduction

Tectonics of the Iranian plateau is especially characterized by active faulting, large destructive earthquakes, Quaternary volcanism and spatial distribution of ore deposits [*Amirihanza et al.,* 2018]. About 180300 human fatalities have been reported due to the occurrence of 217 earthquakes in this region in the period of 1900 to 2020. 17 of these earthquakes, each of which resulted in more than 1000 victims and 15 of them were greater than M_W=7 [NOAA, 2020]. A substantial part of earthquake fatalities is due to tectonic activities along eastern and western margins of the Lut Block, which is considered as a rigid micro-plate with a thin crustal structure [*Dehghani, Makris,* 1984]. The eastern border of this block is the Nehbandan fault system which overprints the Sistan suture zone. The Sistan suture zone represents the closure of the N-S branch of the Neotethys Ocean in the east of Iran. The western border is separated from Central Iran by several N-S and NNW-SSE striking right-lateral fault systems such as the Nayband, the Gowk, the Shahdad, and Lakarkuh [*Hashemi et al.,* 2018].

Thirteen destructive earthquakes from 1977 to 2020 were accompanied by surface rupture with a length of about 207 km in the western border of the Lut Block. These earthquakes resulted in ~44700 human losses with ~36640 injured and more than 100000 homeless. To the best of our knowledge, the significant relationship between the surface evidence of the seismic faults and the depth of earthquakes in this region has not been investigated to determine the accuracy of their mechanism.

Earthquake catalogs and field observations that study several active fault systems and their interactions in some area has been used to determine the tectonic situation [*Derakhshani, Eslami,* 2011; *Nemati, Derakhshani,* 2021; *Rashidi et al.,* 2020]. Therefore, identification of the general seismotectonic pattern may provide complementary deductions for more realistic analysis and interpretation of observations. In this study, the main active faults which include

Nayband, Lakarkuh, Kuhbanan, Davaran, Jorjafk, Gowk, Shahdad, and Anar faults (Fig. 1) were investigated for matching superficial and deep communication.

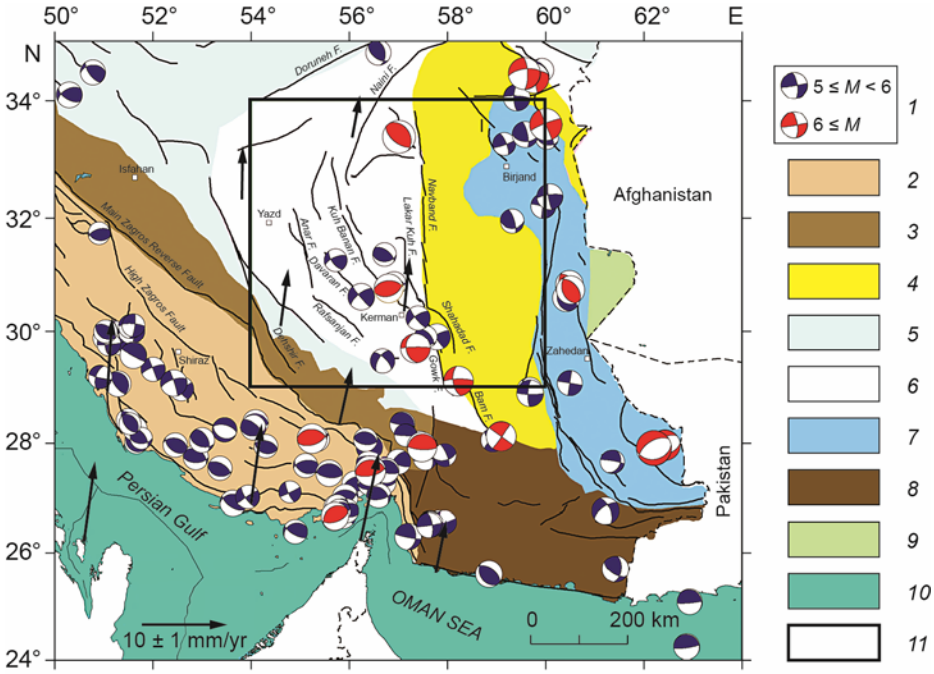

Fig. 1. Tectonic setting of southern Iran

1 – focal mechanisms according to *CMT* (***C****entroid* ***M****oment* ***T****ensor*) for earthquakes with *M*>*5* for the period 1976–2018 (http://www.seismology.harvard.edu/CMTsearch.html) according to [*Kianimehr et al.*, 2018]; *2* – Zagros folded zone; *3* – areas of metamorphism; *4* – Lut Block; *5* – Central Iran; *6* – Tabas and Yazd regions (sub-zone of Central Iran); *7* – East Iranian belt (Sistan suture zone); *8* – Makran-Jazmurian depression; *9* – Zabol block; *10* – water area; *11* – boundaries of the investigated area; arrows – vectors of surface displacement velocities according to GPS data, mm/yr (according to [*Vernant et al.,* 2004] with changes)

Рис. 1. Тектоническая обстановка южного Ирана

1 – механизмы очагов по *CMT* (***C****entroid* ***M****oment* ***T****ensor*) для землетрясений с *M*>5 за период 1976–2018 гг. (http://www.seismology.harvard.edu/CMTsearch.html) по данным [*Kianimehr et al.,* 2018]; *2* – Загросская складчатая зона; *3* – области метаморфизма; *4* – Лутский блок; *5* – Центральный Иран; *6* – области Тебез и Йезд (подзона Центрального Ирана); *7* – Восточно-Иранский пояс (Систанская шовная зона); *8* – впадина Джаз-Муриан-Макран; *9* – Забольский блок; *10* – морская акватория; *11* – границы исследуемой области; стрелки – вектора скоростей смещений поверхности по данным *GPS*, мм/год (по [*Vernant et al.,* 2004] с изменениями)

Material and methods

The main active faults of the study area are investigated using the Quaternary surface landforms, tilting and offset in rock units, and landscape responses to the cumulative displacement of active faults. We combined DEM terrain interpretations, satellite images (acquired from Quickbird, Aster, Landsat, and Google Earth) which have been analyzed using geomorphological field surveys to study the active tectonics of this area. The offset, the upstream and downstream courses of each river, which were projected onto the fault trace, were measured and we estimated river gradients from SRTM data. To understand the depth characteristics of the faults, we used the 4 NE-SW cross-sections (for more information, see below in the section 4 and in Fig. 8, *on the left*) that have been provided perpendicular to the main seismic trend in the area. These cross-sections can indicate the depth range of the earthquake occurrence for the significant faults in the crust. For this purpose, we first updated the seismicity catalog obtained of H. Kianimehr and colleagues [*Kianimehr et al.,* 2018] by merging the catalogs of the Broadband Iranian National Seismic Network (BIN) and Iranian Seismic Center (IRSC) in the period from July 2017 to December 2020, then we deleted the large individual reading errors and finally relocated by regional minimum 1-D model for central Iran.

Strike-slip faults

Nayband fault. The Nayband right-lateral fault runs for roughly 300 km (Fig. 2, *above on the right*) with a sharp linear trace on the surface. Several relatively large displacements can be seen along this fault, including a drainage offset of about 7 km and also more than 7 km offset in Eocene rock formation (Fig. 2, *on the left*).

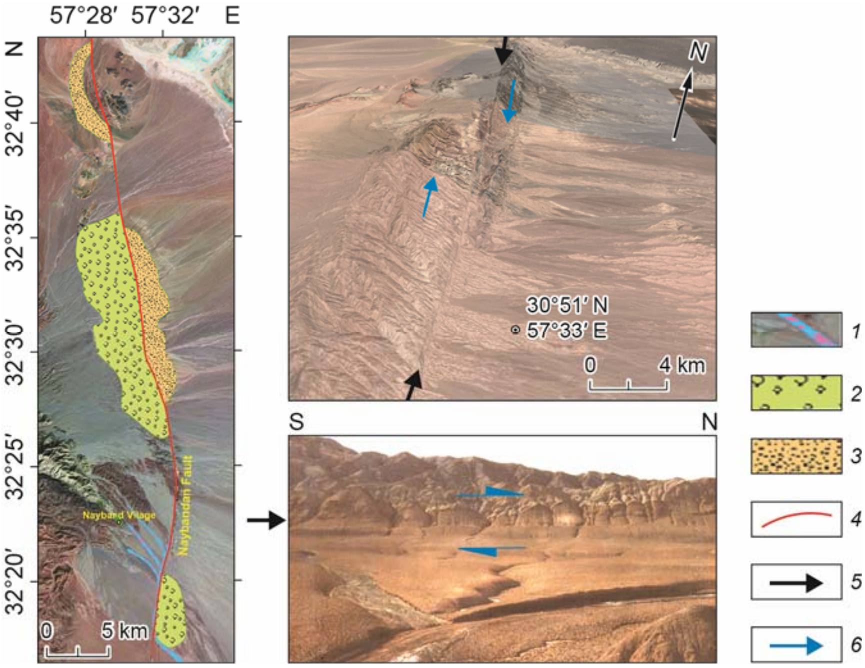

Fig. 2. Nayband fault. *On the left*: image from the *Landsat* satellite. The largest offset of the river is about 7 km, the offset of Eocene rocks is also about 7 km. *On the right*: *3D-Quickbird* satellite image of the fault (according to *Google Earth*), with the right-lateral offset of rocks along the fault (*above*). The point with coordinates is the location of the field survey of river offsets along the fault, which image is given *below*. *1–3* – rocks: *1* – Quaternary (alluvial), *2* – Eocene (volcanic), *3* – Triassic (shale, sandstone); *4*, *5* – fault (*4*) and its trace (*5*); *6* – displacement direction of the fault sides

Рис. 2. Нейбандский разлом. *Слева*: снимок со спутника *Landsat*. Наибольшее смещение реки составляет около 7 км, смещение эоценовых горных пород также ≈7 км. *Справа*: снимок разлома со спутника 3*D-Quickbird* (по данным *Google Earth*), на котором видно правостороннее смещение горных пород вдоль разлома (*вверху*). Точка с координатами – место полевой съемки смещений рек вдоль разлома, фотография которого представлена *внизу*. *1–3* – горные породы: *1* – четвертичные (аллювиальные), *2* – эоценовые (вулканические), *3* – триасовые (сланцы, песчаники); *4*, *5* – разлом (*4*) и его след (*5*); *6* – направление смещения бортов разлома

According to main structural discontinuities such as extensional stepovers and bends, six first-order segments can be identified along the Nayband fault [*Rashidi et al.,* 2018]. These fault segments are arranged in a right-stepping en-echelon pattern, which is obvious in the field, satellite images, and also topographic maps.

Offset fluvial valleys or river channels, including rivers beheaded and deflected by this fault, provide some of the most important geomorphic evidence for the determination of the fault slip sense (see Fig. 2).

Gowk fault. The right-lateral Gowk fault (see Fig. 1) accommodates a major part of 15 mm/yr total of the north-south, right-lateral shearing between Afghanistan and the interior of Iran [*Meyer, Dortz,* 2007; *Vernant et al.,* 2004; *Walker, Jackson,* 2004] which includes five main segments [*Rashidi et al.,* 2018] with a cumulative offset of about 12 km along this system [*Walker, Jackson,* 2002]. Along these segments, the release of right step-overs and pull-apart basins can be observed which have extensively affected the drainage system. Due to the continuous activities of the fault, different offsets in main structures with different ages can be observed (Fig. 3).

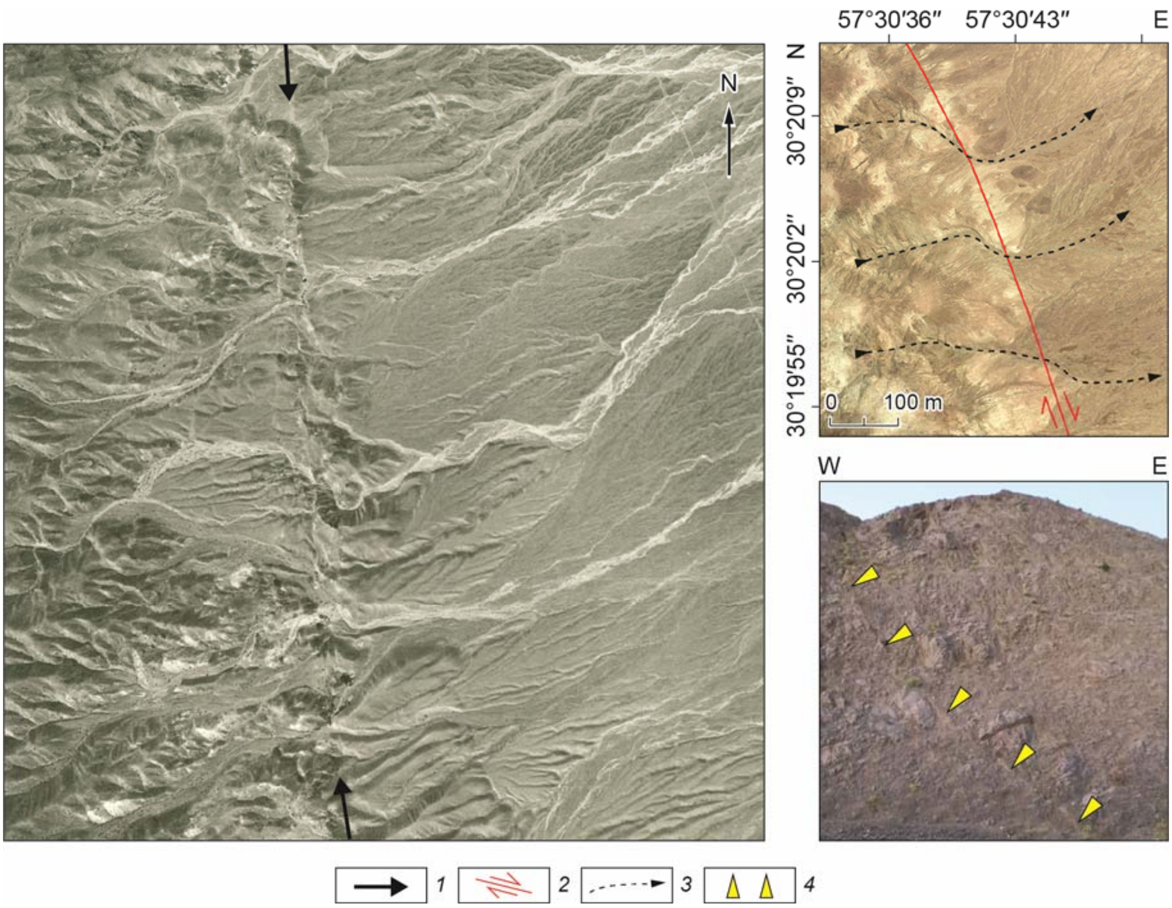

Fig. 3. Gowk fault. Satellite images of the fault (*on the left*) and the river offset of ~100 m (*above on the right*). *Below on the right* – a photograph of the fault in the north of Sirch village. *1* – location of the fault; *2* – fault and directions of offsets of its sides; *3* – watercourses; *4* – the displacement surface

Рис. 3. Разлом Гоук (Gowk). Спутниковые снимки разлома (*слева*) и смещения реки, составляющего ~100 м (*справа вверху*). *Справа внизу* – фотография разлома на севере с. Сирч. *1* – местоположение разлома; *2* – разлом и направления смещения его бортов; *3* – русла водотоков; *4* – поверхность сместителя

Based on radiocarbon dating of two terrestrial wood fragments, R. Walker have estimated a minimum Holocene slip rate of 3.8±0.7 mm/yr on the Gowk fault which seems to import to the northern branches of Kuhbanan, Lakar Kuh, and Nayband faults [Walker et al., 2010]. However, some slip rate is consuming by rotating blocks along this fault but there is no field information about its value. The relatively high slip rate of the Gowk fault infers a high seismic potential which can be deduced also from the number of destructive earthquakes ascribed to that.

Shahdad fault system. The structural style changes along the Shahdad fold-and-thrust belt from the south to the north. The frontal ridge is a linear arc structure that has been developed along the eastern edge of this fold-and-thrust belt. To the north, it has an NW–SE trend, then to the south, it changes to N–S trend (see Fig. 1). The fault-related folding has been well developed and the elevation is relatively larger in the central part of the ridge. The main ridges in this part of the belt are shorter than the frontal ridge where fault plain with slickenlines indicate the reverse component for this fault (Fig. 4, *above on the left*).

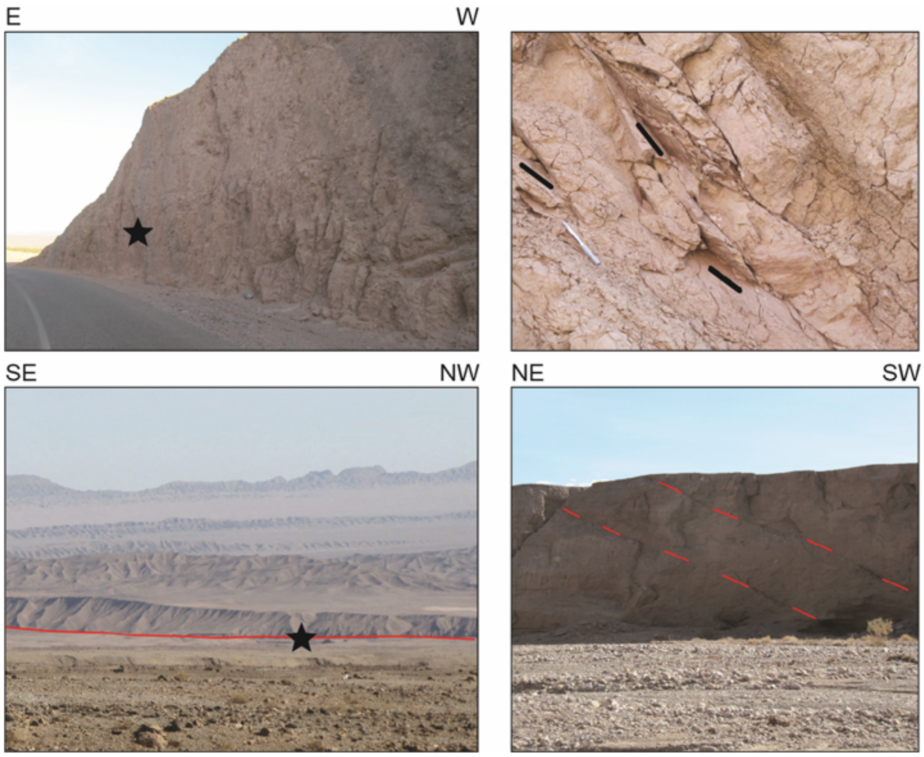

Fig. 4. *Above:* photographs of the Shahdad fault system in the west margin of the Lut Block. *On the left* – layers of Quaternary deposits cut by the fault; *on the right* – slickenlines on the fault plane (black segments – direction of slickenlines). *Below*: photographs of the Lakarkuh fault. *On the left* – thrust of Quaternary sediments along the fault; *on the right* – a fault in Quaternary sediments. The red line is the fault trace in the Quaternary deposits; red dashes – reverse fault surfaces. The asterisks mark the locations of the area shown in the respective photographs to the right

Рис. 4. *Вверху*: фотографии системы разломов Шахдад на западной окраине Лутского блока. *Слева* – слои четвертичных отложений, рассеченные разломом; *справа* – борозды скольжения на плоскости разлома (черные отрезки – направление борозд скольжения). *Внизу*: фотографии разлома Лакаркух. *Слева* – надвиг четвертичных отложений по разлому; *справа* – разлом в четвертичных отложениях. Красная линия – след разлома в четвертичных отложениях; красные штрихи – поверхности надвиговых сместителей. Звездочками отмечены местоположения участков, приведенных на соответствующих фотографиях справа

Lakarkuh fault. The Lakarkuh right-lateral fault runs for about 100 km (see Fig. 1) with a WNW-ESE trend. This fault has been exposed in basin sediments on the western side of the Lakarkuh desert and its dip-slip component in southern branches with NW-SE trend has been formed by shortening in this area (Fig. 4, *below on the left*). The faulting in the south of the Lakarkuh desert has reversed offsets which are visible in the field visit (see Fig. 4, *below on the left*). Moreover, this fault is likely a southern terminal structure to the Lakarkuh fault, which was the cause of the December 2017 Hojedk earthquake.

Kuhbanan fault. The Kuhbanan fault system with a length of ~300 km long and NNW-SSE direction includes some segments with NW-SE trends (see Fig. 1). Bazargan fault, as a segment of the Kuhbanan fault that is located near Kerman city, is considered active according to the morphotectonic features [*Rahbar, Bafti, Derakhshani,* 2017] and shows a reverse mechanism where the Cretaceous limestone was truncated and thrusted on the Jurassic rock units (Fig. 5)

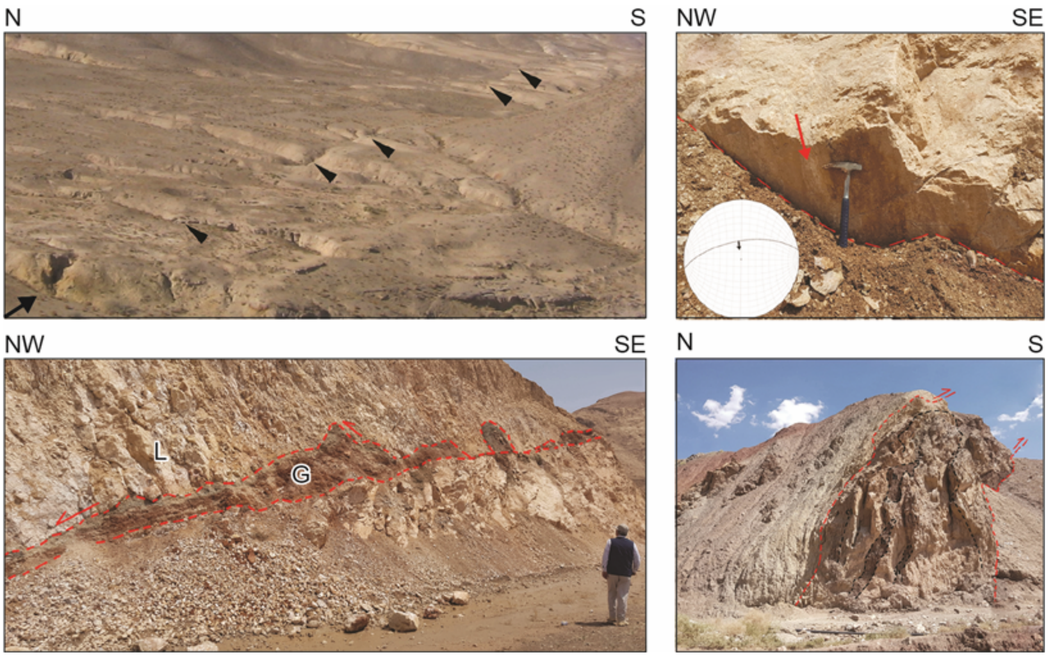

Fig. 5. Photographs of the Kuhbanan fault. *Above on the left*: Fault line (shown by black arrow and triangles) among Quaternary deposits; *below on the left*: cretaceous limestones *L*, truncated and duplicated by the Bazargan thrust – part of the Kuhbanan fault; gouge *G* is visible in the fault zone. *Above on the right*: outcrop view and stereographic projection of the slickenside and slickenlines (marked with a red arrow) of a minor thrust fault near the Bazargan thrust; *below on the right*: intense folding and development of horsetail structures with cleavage in clays and sandstones of the *Bidouie* formation within the strike-slip zone, in the east of the Bazargan village. Red dashed lines and thin red arrows – the Bazargan fault zone and direction of strike-slip along the fault

Рис. 5. Фотографии Кухбананского разлома. *Слева вверху*: линия разлома (показана черной стрелкой и треугольниками) среди четвертичных отложений; *слева внизу*: меловые известняки *L*, усеченные и дублированные Базарганским надвигом – частью Кухбанского разлома; в зоне разлома видна канавка *G*. *Справа вверху*: вид обнажения и стереографическая проекция зеркала и борозд скольжения (отмечены красной стрелкой) надвига младшего порядка рядом с Базарганским надвигом; *справа внизу*: интенсивная складчатость и развитие структур типа “конский хвост” с кливажом в глинах и песчаниках формации *Bidouie* в пределах сдвиго-надвиговой зоны, восточнее с. Базарган. Красные пунктирные линии и тонкие красные стрелки – Базарганская разломная зона и направление сдвига по разлому

Earthquake on November 28, 1933 (M=6.2) ruptured a section of the Kuhbanan fault and destroyed villages to the NW of Behabad. N.N. Ambraseys and C.P. Melville reported 5 km of discontinuous open joints and cracks [*Ambraseys, Melville,* 2005]. Earthquake on December 19, 1977 (M_w=5.8) was accompanied by a rupture ~20 km and a slip of less than 20 cm along this fault as a right-lateral strike-slip system with a reverse component [*Berberian, Asudeh, Arshadi,* 1979]. Numerous streams and rivers show evidence for right-lateral offset along different segments of the Kuhbanan fault [*Kermani, Derakhshani, Bafti*, 2017; *Rashidi et al.,* 2019]. The reversing rock units and fault trace can be observed along the fault (see Fig. 5).

Davaran fault. The Davaran fault with a length of ~200 km is located at the northeast of Rafsanjan [*Mehrabi et al.,* 2019]. This fault has a right-lateral strike-slip mechanism with a reverse component [*Allen et al.,* 2011]. Structural evidence such as right-lateral offsets of drainages in Quaternary units, shutter ridges, and fault traces on satellite images indicate that this fault is active with a large component of shortening (Fig. 6).

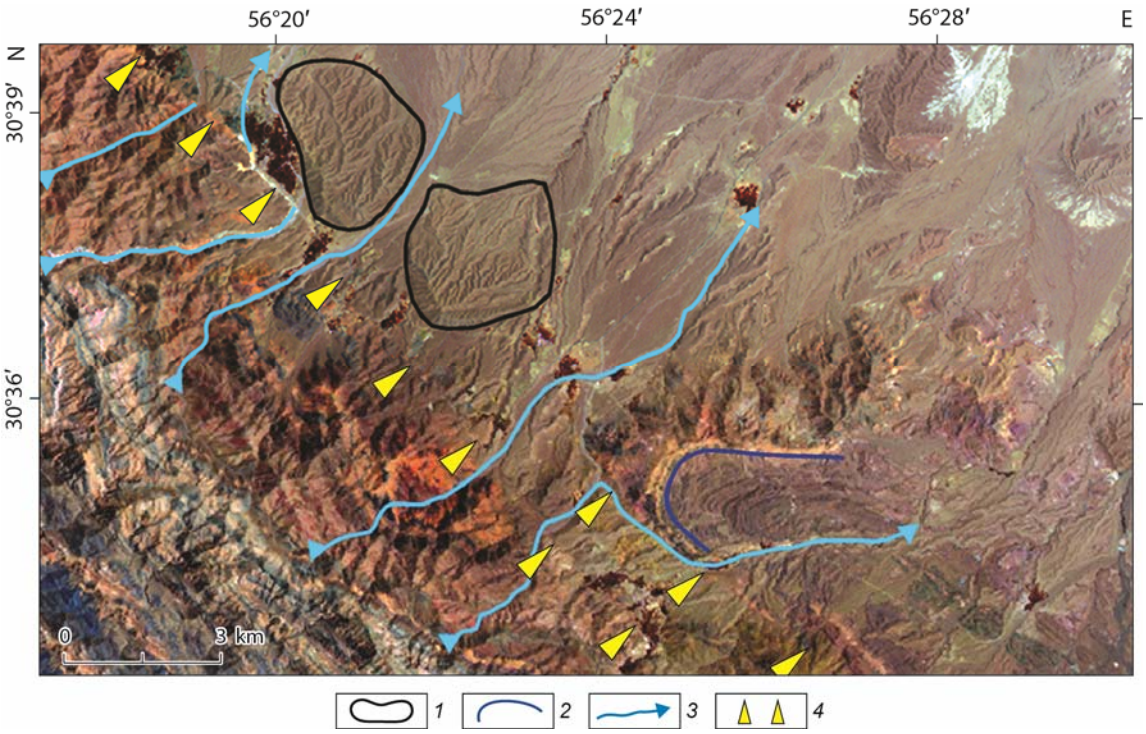

Fig. 6. Davaran fault. Satellite image with marked geomorphological features *1–4*: shutter ridges blocking the drainage (*1*); shear foldings (*2*); displaced watercourses (*3*); rupture traces along the fault (*4*)

Рис. 6. Даваранский разлом. Спутниковый снимок с отмеченными геоморфологическими признаками *1–4*: предсдвиговыми хребтиками, блокирующими дренаж (*1*); сдвиговыми складками (*2*); смещенными руслами водотоков (*3*); следами разрывов вдоль разлома (*4*)

Anar fault. Geomorphic evidence in the Quaternary rock units indicates a high activity of the Anar fault [*Mehrabi et al.,* 2021]. Along its southern part located on the plain, there are traces of active faulting, tilting of young rock units, drag folds, and also fault scarps (Fig. 7). Young rock units in the compressional-shear zone of the Anar fault have been folding. Fault scarps that are visible in the southern part of the Anar fault show more than 8 meters in the vertical uplift (Fig. 7, *below on the right*).

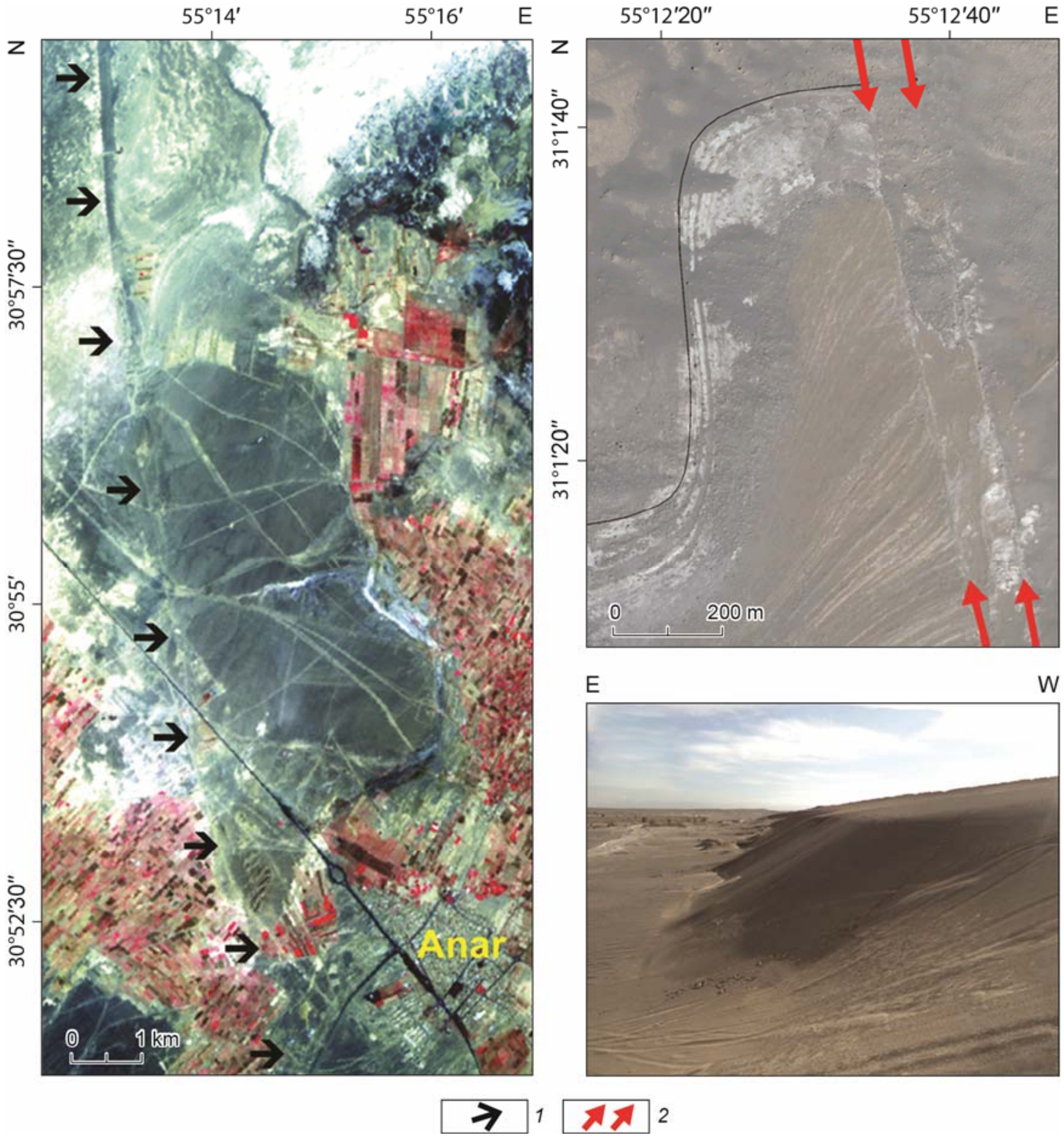

Fig. 7. Anar fault. Satellite images of the surface fault trace (*on the left*) and shear foldings along it (*above on the right*). Photographs of the Anar fault scarp (*below on the right*). *1* – trace of the Anar fault; *2* – fault zone

Рис. 7. Анарский разлом. Спутниковые снимки поверхностного следа разлома (*слева*) и сдвиговых складок вдоль него (*справа вверху*). Фотография уступа Анарского разлома (*справа внизу*). *1* – след Анарского разлома; *2* – разломная зона

Seismicity

The apparent lack of seismicity in the Lut Block may be tentatively attributed to its relative rigidity [*Berberian et al.,* 2001]. The high level of seismicity along the western limits of this block [*Kianimehr et al.,* 2018] is considered as a region of especially high seismic hazard (Fig. 8) [*Ambraseys, Melville,* 2005; *Berberian,* 1976; *Berberian, Yeats,* 1999]. Immediately westward of this high seismic hazard zone, the low level of seismicity corresponds to the low GPS deformation rates [*Khorrami et al.,* 2019; *Masson et al.,* 2007; *Vernant et al.,* 2004].

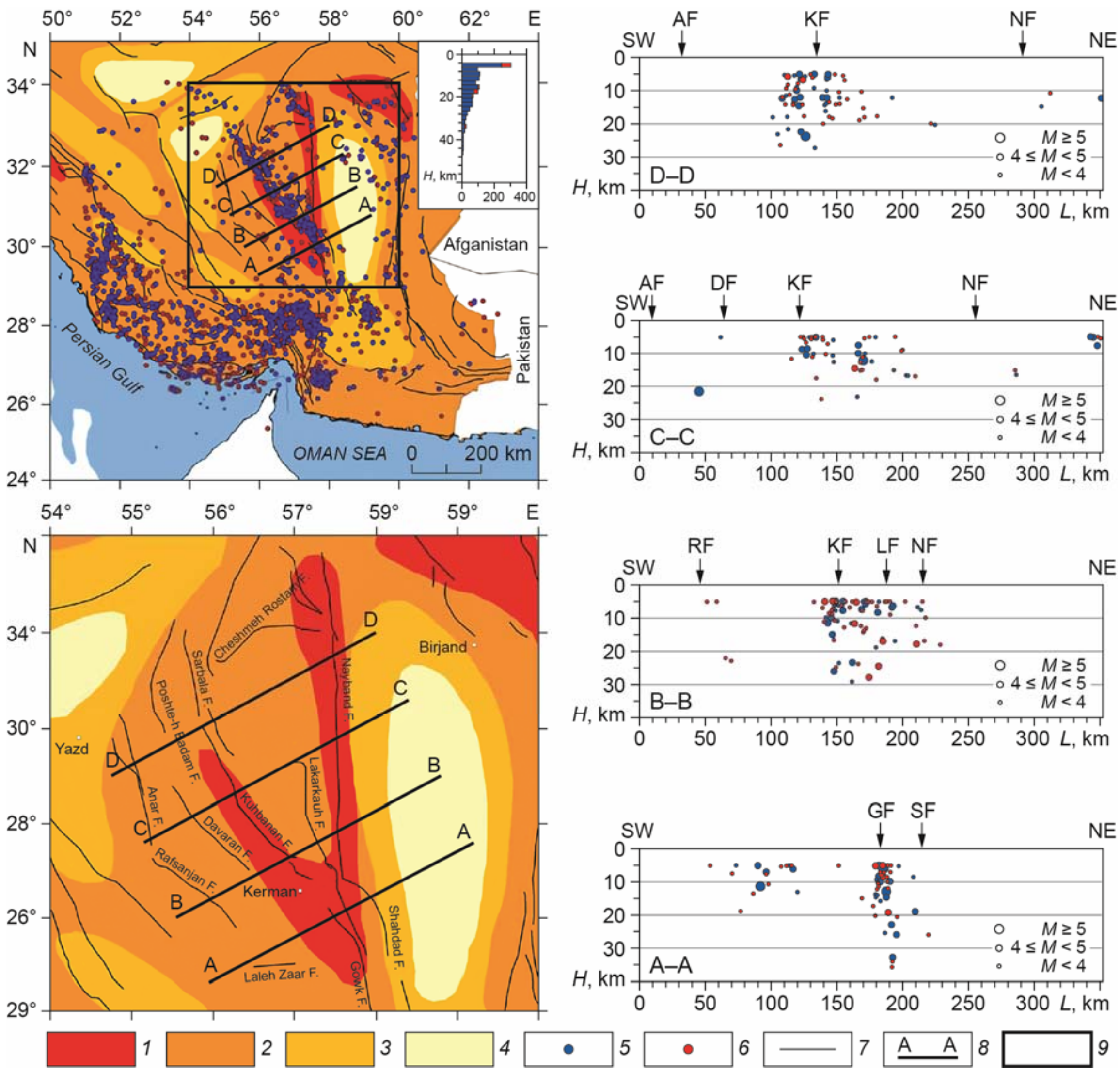

Large earthquakes with different mechanisms (mostly strike-slip) occurred in the east and northeast part of the Lut Block (see Fig. 1). The pattern of seismicity in the east of the Lut Block is diffuse and shows a higher level of seismicity relative to the western part of this block (see Fig. 8) [*Kianimehr et al.,* 2018]. The elongated zone of very high seismic hazard in the middle of Central Iran is following the NW-oriented Kuhbanan fault (see Fig. 8, above on the left). To further assess the correlation between the zone of high seismic activity along the western side of the Lut Block and the mapped major fault systems in the region, we studied 4 SW-NE sections crossing the main trend of seismicity (see Fig. 8, below on the left). These cross-sections (see Fig. 8, on the right) indicate that most earthquakes occurred along known faults in the depth range of 5 km to 20 km in the upper crust. For example, along profile A-A, a cluster dipping almost vertically can be observed which is connected at the surface to Golbaf strike-slip fault system (GF) that appears to play a significant role in transforming the remaining shortening from the South to the North [*Berberian et al.,* 2001]. Most of the deep alignment sections are close to vertical, consistent with dominant strike-slip motion along Golbaf, Kuhbanan, and Posht-e Badam major faults in Central Iran that accommodate additional N-S shortening by counterclockwise rotation in the horizontal plane [*Mattei et al.,* 2012; *Walker, Jackson,* 2004; *Walpersdorf et al.,* 2014].

Fig. 8. Distribution of earthquake hypocenters in comparison with seismic hazard map. *Above on the left*: seismicity map (according to [*Kianimehr et al.,* 2018] with changes). The inset shows the distribution of hypocenter depths (on the horizontal axis – the number of earthquakes *N*). *Below on the left*: seismic hazard map including main fault systems in the western margin of the Lut Block with the location of A-A–D-D profiles. *On the right*: depth distribution of earthquakes along the profiles from bottom to top from profile A-A to profile D-D. Arrows on the upper horizontal axes – the position of the faults: Gowk (GF); Shahdad thrust (SF); Rafsanjan (RF); Kuhbanan (KF); Lakarkuh (LF); Nayband (NF); Anar (AF); Davaran (DF)

1–4 – zones of seismic hazard: very high (*1*), high (*2*), moderate (*3*), low (*4*); *5–6* – well-localized epicenters of events according to data from both (*5*) and only one (*6*) of the used seismic catalogs, respectively (for more details, see [*Kianimehr et al.,* 2018]); *7* – the position of the main faults; *8* – profiles for which the depth distributions of earthquake hypocenters were plotted; *9* – boundaries of the investigated area

Рис. 8. Распределение гипоцентров землетрясений в сравнении с картой сейсмической опасности. *Слева вверху*: карта сейсмичности (по [*Kianimehr et al.,* 2018] с изменениями). На врезке – распределение глубин гипоцентров (на горизонтальной оси – количество землетрясений *N*). *Слева внизу*: карта сейсмической опасности, включающая основные системы разломов на западной окраине Лутского блока с расположением профилей A-A–D-D. *Справа*: распределение землетрясений по глубине по профилям снизу вверх от профиля A-A до профиля D-D. Стрелки на верхних горизонтальных осях – положение разломов: Гоук (GF); надвига Шехдад (SF); Рафсанджанского (RF); Кухбанана (KF); Лакаркух (LF); Нейбандского (NF); Анарского (AF); Даваранского (DF)

1–4 – зоны сейсмической опасности: очень высокая (*1*), высокая (*2*), средняя (*3*), низкая (*4*); *5–6* – хорошо локализуемые эпицентры событий по данным обоих (*5*) и только одного (*6*) из используемых сейсмических каталогов соответственно (подробнее см. в [*Kianimehr et al.,* 2018]); *7* – положение основных разломов; *8* – профили, для которых были построены распределения гипоцентров землетрясений по глубине; *9* – границы исследуемой области

Conclusion

Major fault systems located at the west of the Lut Block generally have two types of right-lateral strike-slip and reverse mechanisms. Most of the alignments' in-depth sections indicated the special role of the strike-slip mechanism in the area. These faults with NS strike include Anar, north part of the Kuhbanan, middle part of Lakarkuh, Nayband and Gowk faults. Depth sections show that other faults such as Rafsanjan, Davaran, the southern part of Kuhbanan, and Shahdad with NW-SE strike have a reverse mechanism in addition to their strike-slip mechanism. Our geomorphological evidence confirms that the right-lateral strike-slip motion along the NS faults has resulted in the shearing and thrusting of the recent rock units along NW-SE and EW faults.

Acknowledgments

Authors are grateful to the editor and reviewers, for their useful comments on the manuscript.

Funding

This work was supported by the International Institute of Earthquake Engineering and Seismology (IIEES).

Conflict of interest

The authors declare they have no conflict of interest

References

Allen M.B., Kheirkhah M., Emami M.H., Jones S.J., Right-lateral shear across Iran and kinematic change in the Arabia–Eurasia collision zone, *Geophysical Journal International*, 2011, vol. 184, no. 2, pp. 555-574. DOI: https://doi.org/10.1111/j.1365-246X.2010.04874.x

Ambraseys N.N., Melville C.P., *A history of Persian earthquakes*, Cambridge: Cambridge university press, 2005, 240 p.

Amirihanza H., Shafieibafti S., Derakhshani R., Khojastehfar S., Controls on Cu mineralization in central part of the Kerman porphyry copper belt, SE Iran: constraints from structural and spatial pattern analysis, *Journal of Structural Geology*, 2018, vol. 116, pp. 159-77. https://doi.org/10.1016/j.jsg.2018.08.010

Berberian M., *Contribution to the seismotectonics of Iran. Part II*, Tehran: Geol. Survey of Iran, 1976, 518 p.

Berberian M., Yeats R.S., Patterns of historical earthquake rupture in the Iranian Plateau, *Bulletin of the Seismological society of America*, 1999, vol. 89, no. 1, pp. 120-139.

Berberian M., Asudeh I., Arshadi S., Surface rupture and mechanism of the Bob-Tangol (southeastern Iran) earthquake of 19 December 1977, *Earth and Planetary Science Letters*, 1979, vol. 42, no. 3, pp. 456-462. DOI: https://doi.org/10.1016/0012-821X(79)90055-4

Berberian M., Jackson J., Fielding E., Parsons B.E., Priestley K., Qorashi M., Talebian M., Walker R., Wright T.J., Baker C., The 1998 March 14 Fandoqa earthquake (Mw 6.6) in Kerman province, southeast Iran: re-rupture of the 1981 Sirch earthquake fault, triggering of slip on adjacent thrusts and the active tectonics of the Gowk fault zone, *Geophysical Journal International*, 2001, vol. 146, no. 2, pp. 371-398. DOI: 10.1046/j.1365-246x.2001.01459.x

Dehghani G., Makris J., The gravity field and crustal structure of Iran, *Neues Jahrbuch für Geologie und Paläontologie-Abhandlungen*, 1984, vol. 168, pp. 215-229. DOI: https://doi.org/10.1127/njgpa/168/1984/215

Derakhshani R., Eslami S., A new viewpoint for seismotectonic zoning, *American Journal of Environmental Sciences*, 2011, vol. 7, no. 3, pp. 212-218. DOI: http://dx.doi.org/10.3844/ajessp.2011.212.218

Hashemi F., Derakhshani R., Bafti S.S., Raoof A., Morphometric dataset of the alluvial fans at the southern part of Nayband fault, Iran, *Data in Brief*, 2018, vol. 21, pp. 1756-1763. DOI: https://doi.org/10.1016/j.dib.2018.11.017

Kermani A.F., Derakhshani R., Bafti S.S., Data on morphotectonic indices of Dashtekhak district, Iran, *Data in brief*, 2017, vol. 14, pp. 782-788. DOI: https://doi.org/10.1016/j.dib.2017.08.052

Khorrami F., Vernant P., Masson F., Nilfouroushan F., Mousavi Z., Nankali H., Saadat S.A., Walpersdorf A., Hosseini S., Tavakoli P., Aghamohammadi A., Alijanzade M., An up-to-date crustal deformation map of Iran using integrated campaign-mode and permanent GPS velocities, *Geophysical Journal International*, 2019, vol. 217, no. 2, pp. 832-843. DOI: https://doi.org/10.1093/gji/ggz045

Kianimehr H., Kissling E., Yaminifard F., Tatar M., Regional minimum 1-D P-wave velocity model for a new seismicity catalogue with precise and consistent earthquake locations in southern Iran, *Journal of seismology*, 2018, vol. 22, no. 6, pp. 1529-1547. DOI: https://doi.org/10.1007/s10950-018-9783-4

Masson F., Anvari M., Djamour Y., Walpersdorf A., Tavakoli F., Daignieres M., Nankali H., Gorp S.V., Large-scale velocity field and strain tensor in Iran inferred from GPS measurements: new insight for the present-day deformation pattern within NE Iran, *Geophysical Journal International*, 2007, vol. 170, no. 1, pp. 436-440. DOI: https://doi.org/10.1111/j.1365-246X.2007.03477.x

Mattei M., Cifelli F., Muttoni G., Zanchi A., Berra F., Mossavvari F., Eshraghi S.A., Neogene block rotation in central Iran: Evidence from paleomagnetic data, *Bulletin*, 2012, vol. 124, no. 5-6, pp. 943-956. DOI: https://doi.org/10.1130/B30479.1

Mehrabi A., Khabazi M., Almodaresi S.A., Nohesara M., Derakhshani R., Land use changes monitoring over 30 years and prediction of future changes using multi-temporal Landsat imagery and the land change modeler tools in Rafsanjan city (Iran), *Sustainable Development of Mountain Territories*, 2019, vol. 11, no. 1, pp. 26-35. DOI: https://doi.org/10.21177/1998-4502-2019-11-1-26-35

Mehrabi A., Pirasteh S., Rashidi A., Pourkhosravani M., Derakhshani R., Liu G., Mao W., Xiang W., Incorporating Persistent Scatterer Interferometry and Radon Anomaly to Understand the Anar Fault Mechanism and Observing New Evidence of Intensified Activity, *Remote Sensing*, 2021, vol. 13, no. 11, pp. 2072. DOI: https://doi.org/10.3390/rs13112072

Meyer B., Dortz K.L., Strike-slip kinematics in central and eastern Iran: Estimating fault slip-rates averaged over the Holocene, *Tectonics*, 2007, vol. 26, TC5009. DOI: https://doi.org/10.1029/2006TC002073

Nemati M., Derakhshani R., Short-term seismicity patterns along the most active faults in Iran, *Journal of Iberian Geology*, 2021, vol. 47, no. 3, pp. 441-459.

National Geophysical Data Center / World Data Service (NGDC/WDS): NCEI/WDS Global Significant Earthquake Database. Ashville: NOAA National Centers for Environmental Information. 2020. DOI: https://doi.org/10.7289/V5TD9V7K

Rahbar R., Bafti S.S., Derakhshani R., Investigation of the tectonic activity of Bazargan Mountain in Iran, *Sustainable Development of Mountain Territories*, 2017, vol. 9, no. 4, pp. 380-386. DOI: http://dx.doi.org/10.21177/1998-4502-2017-9-4-380-386

Rashidi A., Abbassi M.R., Nilfouroushan F., Shafiei S., Derakhshani R., Nemati M., Morphotectonic and earthquake data analysis of interactional faults in Sabzevaran Area, SE Iran, *Journal of Structural Geology*, 2020, vol. 139, Art. ID 104147. DOI: https://doi.org/10.1016/ j.jsg.2020.104147

Rashidi A., Khatib M.M., Nilfouroushan F., Derakhshani R., Mousavi S.M., Kianimehr H., Djamour Y., Strain rate and stress fields in the West and South Lut Block, Iran: Insights from the inversion of focal mechanism and geodetic data, *Tectonophysics*, 2019, vol. 766, pp. 94-114. DOI: https://doi.org/10.1016/j.tecto.2019.05.020

Rashidi A., Khatib M.M., Raeesi M., Mousavi S.M., Djamour Y., Geometric-kinematic characteristics of the main faults in the W-SW of the Lut Block (SE Iran), *Journal of African Earth Sciences*, 2018, vol. 139, pp. 440-462. DOI: https://doi.org/10.1016/j.jafrearsci.2017.12.027

Vernant P., Nilforoushan F., Hatzfeld D., Abbassi M., Vigny C., Masson F., Nankali H., Martinod J., Ashtiani A., Bayer R., Tavakoli F., Chéry J., Present-day crustal deformation and plate kinematics in the Middle East constrained by GPS measurements in Iran and northern Oman, *Geophysical Journal International*, 2004, vol. 157, no. 1, pp. 381-398. DOI: https://doi.org/10.1111/j.1365-246X.2004.02222.x

Walker R., Jackson J., Offset and evolution of the Gowk fault, SE Iran: a major intra-continental strike-slip system, *Journal of Structural Geology*, 2002, vol. 24, no. 11, pp. 1677-1698. DOI: 10.1016/S0191-8141(01)00170-5

Walker R., Jackson J., Active Tectonics and Late Cenozoic Strain Distribution in Central and Eastern Iran, *Tectonics*, 2004, vol. 23, issue 5. DOI: https://doi.org/10.1029/2003TC001529

Walker R., Talebian M., Sloan R., Rasheedi A., Fattahi M., Bryant C., Holocene slip-rate on the Gowk strike-slip fault and implications for the distribution of tectonic strain in eastern Iran, *Geophysical Journal International*, 2010, vol. 181, no. 1, pp. 221-228. DOI: https://doi.org/10.1111/j.1365-246X.2010.04538.x

Walpersdorf A., Manighetti I., Mousavi Z., Tavakoli F., Vergnolle M., Jadidi A., Hatzfeld D., Aghamohammadi A., Bigot A., Djamour Y., Nankali H., Sedighi M., Present-day kinematics and fault slip rates in eastern Iran, derived from 11 years of GPS data, Jo*urnal of Geophysical Research*: *Solid Earth*, 2014, vol. 119, no. 2, pp. 1359-1383. DOI: https://doi.org/10.1002/2013JB010620

About the authors

RASHIDI Ahmad – Dr. Sci. (Geo.), Assistant Professor, International Institute of Earthquake Engineering and Seismology (IIEES). Tehran, 19537-14453, Iran. Ph.: +98(21) 22830830. E-mail: rashidi@iiees.ac.ir

KIANIMEHR Hossein – Dr. Researcher, Iranian Seismological Center, Institute of Geophysics, University of Tehran. Tehran, 14155-6466, Iran. Ph.: +98(21) 88028161. E-mail: kianimehrhossein@ut.ac.ir

SHAFIEIBAFTI Shahram – Dr. Sci. (Geo.), Associate Professor, Shahid Bahonar University of Kerman. Kerman, 76169-14111, Iran. Ph.: +98 (34) 33257435. E-mail: shafiei_shahram@uk.ac.ir

MEHRABI Ali – Dr. Sci. (Geo.), Assistant Professor, Shahid Bahonar University of Kerman. Kerman, 76169-14111, Iran. Ph.: +98(34) 33257435. E-mail: mehrabi@uk.ac.ir

DERAKHSHANI Reza – Dr. Sci. (Geo.), Associate Professor, Shahid Bahonar University of Kerman. Kerman, 76169-14111, Iran; Utrecht University. Heidelberglaan 8, 3584 CS Utrecht, Netherlands. Ph.: +31(30) 253-51-12. E-mail: r.derakhshani@uu.nl

АКТИВНЫЕ РАЗЛОМЫ ЗАПАДНОЙ ЧАСТИ ЛУТСКОГО БЛОКА (ЦЕНТРАЛЬНЫЙ ИРАН)

А. Рашиди[1], Х. Кианимер[2], Ш. Шафиэйбафти[3], А. Мераби[3], Р. Дерахшани[3,4]

[1] *Международный институт сейсмостойкого строительства и сейсмологии, Тегеран, Иран*
[2] *Иранский сейсмологический центр, Институт геофизики, Тегеранский университет, Тегеран, Иран*
[3] *Керманский университет Шахида Бахонара, Керман, Иран*
[4] *Утрехтский университет, Утрехт, Нидерланды*
Авторы для переписки: А. Рашиди (e-mail: rashidi@iiees.ac.ir) и Р. Дерахшани (e-mail: r.derakhshani@uu.nl)

Аннотация. Западная окраина Лутского блока, на юго-востоке Ирана, пережила много исторических и зарегистрированных в инструментальный период разрушительных землетрясений, тринадцать из которых в период с 1977 по 2020 гг. сопровождались разрывами суммарной длиной около 207 км. В предлагаемом исследовании указаны свидетельства активной тектонической деятельности основных разломов на основе интерпретации данных цифровой модели рельефа, а также совместного анализа спутниковых и полевых данных. Проанализированы поверхностные признаки, связанные с активностью разломов и их глубинными характеристиками. Представленные результаты геометрическо-кинематической характеристики разломов могут быть использованы для описания сдвиговых разломов, развития свободных и ограничивающих изгибов в положительных структурах "цветка".

Ключевые слова: активные разломы, сейсмическая активность, геоморфологические признаки, свободные и ограничивающие изгибы, Центральный Иран.

Благодарности

Авторы выражают благодарность редактору и рецензентам за их полезные комментарии к рукописи.

Финансирование

Исследование выполнено при поддержке Международного института сейсмической инженерии и сейсмологии (*IIEES*).

Конфликт интересов

Авторы заявляют об отсутствии конфликта интересов.

Литература

Allen M.B., Kheirkhah M., Emami M.H., Jones S.J. Right-lateral shear across Iran and kinematic change in the Arabia–Eurasia collision zone // Geophysical Journal International. 2011. V. 184, N 2. P.555–574. DOI: https://doi.org/10.1111/j.1365-246X.2010.04874.x

Ambraseys N.N., Melville C.P. A history of Persian earthquakes. Cambridge: Cambridge university press, 2005. 240 p.

Amirihanza H., Shafieibafti S., Derakhshani R., Khojastehfar S. Controls on Cu mineralization in central part of the Kerman porphyry copper belt, SE Iran: constraints from structural and spatial pattern analysis // Journal of Structural Geology. 2018. V. 116. P.159–77. DOI: https://doi.org/10.1016/ j.jsg.2018.08.010

Berberian M. Contribution to the seismotectonics of Iran. Part II. Tehran: Geol. Survey of Iran, 1976. 518 p.

Berberian M., Yeats R.S. Patterns of historical earthquake rupture in the Iranian Plateau // Bulletin of the Seismological society of America. 1999. V. 89, N 1. P.120–139.

Berberian M., Asudeh I., Arshadi S. Surface rupture and mechanism of the Bob-Tangol (southeastern Iran) earthquake of 19 December 1977 // Earth and Planetary Science Letters. 1979. V. 42, N 3. P.456–462. DOI: https://doi.org/10.1016/0012-821X(79)90055-4

Berberian M., Jackson J., Fielding E., Parsons B.E., Priestley K., Qorashi M., Talebian M., Walker R., Wright T.J., Baker C. The 1998 March 14 Fandoqa earthquake (Mw 6.6) in Kerman province, southeast Iran: re-rupture of the 1981 Sirch earthquake fault, triggering of slip on adjacent thrusts and the active tectonics of the Gowk fault zone // Geophysical Journal International. 2001. V. 146, N 2. P.371–398. DOI: 10.1046/ j.1365-246x.2001.01459.x

Dehghani G., Makris J. The gravity field and crustal structure of Iran // Neues Jahrbuch für Geologie und Paläontologie-Abhandlungen. 1984. V. 168. P.215–229. DOI: https://doi.org/10.1127/njgpa/168/1984/215

Derakhshani R., Eslami S. A new viewpoint for seismotectonic zoning // American Journal of Environmental Sciences. 2011. V. 7, N 3. P.212–218. DOI: http://dx.doi.org/10.3844/ ajessp.2011.212.218

Hashemi F., Derakhshani R., Bafti S.S., Raoof A. Morphometric dataset of the alluvial fans at the southern part of Nayband fault, Iran // Data in Brief. 2018. V. 21. P.1756–1763. DOI: https://doi.org/10.1016/ j.dib.2018.11.017

Kermani A.F., Derakhshani R., Bafti S.S. Data on morphotectonic indices of Dashtekhak district, Iran // Data in brief. 2017. V. 14. P.782–788. DOI: https://doi.org/10.1016/j.dib.2017.08.052

Khorrami F., Vernant P., Masson F., Nilfouroushan F., Mousavi Z., Nankali H., Saadat S.A., Walpersdorf A., Hosseini S., Tavakoli P., Aghamohammadi A., Alijanzade M. An up-to-date crustal deformation map of Iran using integrated campaign-mode and permanent GPS velocities // Geophysical Journal International. 2019. V. 217, N 2. P.832–843. DOI: https://doi.org/10.1093/ gji/ggz045

Kianimehr H., Kissling E., Yaminifard F., Tatar M. Regional minimum 1-D P-wave velocity model for a new seismicity catalogue with precise and consistent earthquake locations in southern Iran // Journal of seismology. 2018. V. 22, N 6. P.1529–1547. DOI: https://doi.org/10.1007/s10950-018-9783-4

Masson F., Anvari M., Djamour Y., Walpersdorf A., Tavakoli F., Daignieres M., Nankali H., Gorp S.V. Large-scale velocity field and strain tensor in Iran inferred from GPS measurements: new insight for the present-day deformation pattern within NE Iran // Geophysical Journal International. 2007. V. 170, N 1. P.436–440. DOI: https://doi.org/10.1111/j.1365-246X.2007.03477.x

Mattei M., Cifelli F., Muttoni G., Zanchi A., Berra F., Mossavvari F., Eshraghi S.A. Neogene block rotation in central Iran: Evidence from paleomagnetic data // Bulletin. 2012. V. 124, N 5-6. P.943–956. DOI: https://doi.org/10.1130/B30479.1

Mehrabi A., Khabazi M., Almodaresi S.A., Nohesara M., Derakhshani R. Land use changes monitoring over 30 years and prediction of future changes using multi-temporal Landsat imagery and the land change modeler tools in Rafsanjan city (Iran) // Sustainable Development of Mountain Territories. 2019. V. 11, N 1. P.26–35. DOI: https://doi.org/10.21177/1998-4502-2019-11-1-26-35

Mehrabi A., Pirasteh S., Rashidi A., Pourkhosravani M., Derakhshani R., Liu G., Mao W., Xiang W. Incorporating Persistent Scatterer Interferometry and Radon Anomaly to Understand the Anar Fault Mechanism and Observing New Evidence of Intensified Activity // Remote Sensing. 2021. V. 13, N 11. P.2072. DOI: https://doi.org/10.3390/rs13112072

Meyer B., Dortz K.L. Strike-slip kinematics in central and eastern Iran: Estimating fault slip-rates averaged over the Holocene // Tectonics. 2007. V. 26. TC5009. DOI: https://doi.org/10.1029/2006TC002073

Nemati M., Derakhshani R. Short-term seismicity patterns along the most active faults in Iran // Journal of Iberian Geology. 2021. V. 47, N 3. P.441–459. DOI: https://doi.org/10.1007/s41513-020-00133-0

National Geophysical Data Center / World Data Service (NGDC/WDS): NCEI/WDS Global Significant Earthquake Database. Ashville: NOAA National Centers for Environmental Information. 2020. DOI: https://doi.org/10.7289/V5TD9V7K

Rahbar R., Bafti S.S., Derakhshani R. Investigation of the tectonic activity of Bazargan Mountain in Iran // Sustainable Development of Mountain Territories. 2017. V. 9, N 4. P.380–386. DOI: http://dx.doi.org/10.21177/1998-4502-2017-9-4-380-386

Rashidi A., Abbassi M.R., Nilfouroushan F., Shafiei S., Derakhshani R., Nemati M. Morphotectonic and earthquake data analysis of interactional faults in Sabzevaran Area, SE Iran // Journal of Structural Geology. 2020. V. 139. 104147. DOI: https://doi.org/10.1016/j.jsg.2020.104147

Rashidi A., Khatib M.M., Nilfouroushan F., Derakhshani R., Mousavi S.M., Kianimehr H., Djamour Y. Strain rate and stress fields in the West and South Lut Block, Iran: Insights from the inversion of focal mechanism and geodetic data // Tectonophysics. 2019. V. 766. P.94–114. DOI: https://doi.org/10.1016/j.tecto.2019.05.020

Rashidi A., Khatib M.M., Raeesi M., Mousavi S.M., Djamour Y. Geometric-kinematic characteristics of the main faults in the W-SW of the Lut Block (SE Iran) // Journal of African Earth Sciences. 2018. V. 139. P.440–462. DOI: https://doi.org/10.1016/j.jafrearsci.2017.12.027

V*ernant P., Nilforoushan F., Hatzfeld D., Abbassi M., Vigny C., Masson F., Nankali H., Martinod J., Ashtiani A., Bayer R., Tavakoli F., Chéry J.* Present-day crustal deformation and plate kinematics in the Middle East constrained by GPS measurements in Iran and northern Oman // Geophysical Journal International. 2004. V. 157, N 1. P.381–398. DOI: https://doi.org/10.1111/j.1365-246X.2004.02222.x

Walker R., Jackson J. Offset and evolution of the Gowk fault, SE Iran: a major intra-continental strike-slip system // Journal of structural Geology. 2002. V. 24, N 11. P.1677–1698. DOI: 10.1016/S0191-8141(01)00170-5

Walker R., Jackson J. Active Tectonics and Late Cenozoic Strain Distribution in Central and Eastern Iran // Tectonics. 2004. V. 23, Issue 5. DOI: https://doi.org/10.1029/2003TC001529

Walker R., Talebian M., Sloan R., Rasheedi A., Fattahi M., Bryant C. Holocene slip-rate on the Gowk strike-slip fault and implications for the distribution of tectonic strain in eastern Iran // Geophysical Journal International. 2010. V. 181, N 1. P.221–228. DOI: https://doi.org/10.1111/ j.1365-246X.2010.04538.x

Walpersdorf A., Manighetti I., Mousavi Z., Tavakoli F., Vergnolle M., Jadidi A., Hatzfeld D., Aghamohammadi A., Bigot A., Djamour Y., Nankali H., Sedighi M. Present-day kinematics and fault slip rates in eastern Iran, derived from 11 years of GPS data // Journal of Geophysical Research: Solid Earth. 2014. V. 119, N 2. P.1359–1383. DOI: https://doi.org/10.1002/ 2013JB010620

Сведения об авторах

РАШИДИ Ахмад – доктор геологических наук, доцент, Международный институт сейсмостойкого строительства и сейсмологии (IIEES). Тегеран, 19537-14453, Иран. Тел.: +98(21) 22830830. E-mail: rashidi@iiees.ac.ir

КИАНИМЕР Хоссейн – главный научный сотрудник, Иранский сейсмологический центр, Институт геофизики, Тегеранский университет. Тегеран, 14155-6466, Иран. Тел.: +98(21) 88028161. E-mail: kianimehrhossein@ut.ac.ir

ШАФИЭЙБАФТИ Шахрам – доктор геологических наук, доцент кафедры, Керманский университет Шахида Бахонара. Керман, 76169-14111, Иран. Тел.: +98(34) 33257435. E-mail: shafiei_shahram@uk.ac.ir

МЕРАБИ Али – доктор геологических наук, доцент, Керманский университет Шахида Бахонара. Керман, 76169-14111, Иран. Тел.: +98(34) 33257435. E-mail: mehrabi@uk.ac.ir

ДЕРАХШАНИ Реза – доктор геологических наук, доцент кафедры, Керманский университет Шахида Бахонара. Керман, 76169-14111, Иран; Утрехтский университет. Гейдельберглан 8, 3584 CS Утрехт, Нидерланды. Тел.: +31(30) 253-51-12. E-mail: r.derakhshani@uu.nl